Journal of Metals, Materials and Minerals, 35(2), e2184, 2025

High-binding affinity nanobody against SARS-CoV-2 XBB.1.5: Computational-based protein engineering

Phoomintara LONGSOMPURANA[1], Napat KONGTAWORN[2], Rungtiva P. POO-ARPORN[1], and Thanyada RUNGROTMONGKOL[2,3,*]

[1] *Biological Engineering Program, Faculty of Engineering, King Mongkut's University of Technology Thonburi, Bangkok, 10140 Thailand*
[2] *Program in Bioinformatics and Computational Biology, Graduate School, Chulalongkorn University, Bangkok, 10330 Thailand*
[3] *Center of Excellence in Biocatalyst and Sustainable Biotechnology, Department of Biochemistry, Faculty of Science, Chulalongkorn University, Bangkok, 10330 Thailand*

***Corresponding author e-mail**: Thanyada.r@chula.ac.th

Received date:
16 October 2024
Revised date:
28 November 2024
Accepted date:
3 April 2025

Keywords:
Computational-based protein engineering;
HDOCK;
Nanobody;
SARS-CoV-2 XBB.1.5

Abstract

The emergence of the SARS-CoV-2 variant XBB.1.5 has triggered a global health crisis by enhancing viral entry into cells via its spike protein. This study addresses the urgent need to develop neutralizing nanobodies (Nbs) to counteract the SARS-CoV-2 virus. Our aim was to identify a lead Nb and enhance its binding affinity to the receptor-binding motif (RBM) on the receptor-binding domain (RBD) of the SARS-CoV-2 spike protein (S-protein) using computational methods. A total of 29 Nbs were screened against the XBB.1.5 RBD using the HDOCK server to select a lead Nb. This investigation revealed that Nb_7KGK exhibited the highest binding affinity. Subsequently, unfavorable residues of Nb_7KGK were mutated to further enhance binding affinity. As expected, aromatic residues (tyrosine, tryptophan, histidine) were primarily mutated to improve binding affinity, resulting in a new Nb variant named Nb_7KGK(7), with heightened affinity. The engineered Nb_7KGK(7) demonstrated improved chemical interactions with the RBD. Predicted physicochemical properties, such as pI value, total charge, Clashscore, and MolProbity score of the engineered Nb, were also improved. This study highlights the potential of computational design as a preliminary step toward developing effective Nbs against the emerging SARS-CoV-2 XBB.1.5 variant.

1. Introduction

The appearance of the SARS-CoV-2 variant XBB.1.5 has instigated a global health crisis by exploiting the attachment mechanism of its spike protein, facilitating viral entry into cells. Sharma *et al.* [1] conducted a structural analysis that revealed five mutations in the loop region of XBB.1.5 compared to the wild-type (WT): S477N, T478K, E484A, S486P, and F490S, along with a disulfide bond between residues C480 and C488. They performed 1-μs molecular dynamics (MD) simulations on the receptor-binding domain (RBD) of XBB.1.5. To study the reorientation of the RBD loop, the distance between two specific residues was calculated over time: residue 449 (outside the loop) and residue 486 (S486P, within the loop). The mutations in XBB.1.5 alter the interaction patterns, leading to a reorientation of the RBD loop region (residues 470-491, including S486P). This reorientation allows the loop to form more hydrogen bonds with ACE2 compared to the Omicron variant [1]. The S486P mutation enhances the structural flexibility of the spike protein, facilitating its transition between closed and open conformations—critical for effective ACE2 binding. This mutation significantly increases the binding affinity of the XBB.1.5 spike protein to the human ACE2 receptor, with a dissociation constant (K_D) of 3.4 nM, reflecting a much stronger binding affinity compared to XBB.1 and BQ.1.1. These structural changes, driven by the S486P mutation, enhance the virus's ability to spread, potentially leading to new waves of infection [2]. Additionally, this mutation enables the virus to evade neutralization by several monoclonal antibodies [3].

This challenge has inspired an urgent demand for the development of neutralizing molecules to counter viral invasion [4,5]. Antibody (Ab) is well-known to neutralize SARS-CoV-2 by binding to its spike protein, preventing virus entry into cells and subsequent infection [6]. However, antibody neutralization can be less effective against new SARS-CoV-2 variants due to mutations that reduce antibody binding efficacy [7,8]. Moreover, therapeutic monoclonal antibodies can be expensive and challenging to produce at scale, limiting their accessibility and widespread use [9]. Alternatively, nanobodies (Nbs), which are the single-variable heavy chain domains of antibodies [10], are a promising option due to their small size, high binding affinity, solubility, stability, and effectiveness in neutralizing SARS-CoV-2 by binding to its spike protein [11]. Nbs are considered the most promising tools for SARS-CoV-2 neutralization compared to miniproteins, affibodies, affimers, and monobodies due to their small size and unique combination of structural, functional, and application advantages. Nbs, which are the small antibody fragments (12 kDa to 15 kDa) [12], have a size that allows them to specifically bind receptor-binding motif (RBM) epitopes, which are often mutated residues on the receptor-binding domain (RBD) of the SARS-CoV-2 spike protein in many variants. While other

small proteins, such as miniproteins (1 kDa to 10 kDa) [13], affibodies (<10 kDa) [14], affimers (11 kDa) [15], and monobodies (10 kDa) [16], are smaller than Nbs, they may not be as suitable for interacting with the RBM of the RBD. In contrast, Nbs can specifically neutralize the virus at nanomolar to picomolar concentrations, often outperforming other engineered scaffolds in neutralization assays [17]. In terms of application, nanobodies offer significant advantages in stability and functionality. However, challenges remain in optimizing their production and application. Efforts are ongoing to further enhance their stability through computational modeling and engineering, which could expand their use in extreme environments and broaden their therapeutic potential [17]. Additionally, Nbs have demonstrated cross-neutralization capabilities against multiple SARS-CoV-2 variants, including Alpha, Delta, and Omicron subvariants [18,19].

However, traditional methods for Nbs screening, such as phage display and immunization of animals (e.g., camelids), have several drawbacks. These include being time-consuming, costly, resource-intensive, necessitating extensive gene library construction, and requiring expertise in molecular biology techniques [20-22]. To address these limitations, we propose an *in silico* approach to select a Nb and improve its binding affinity with the SARS-CoV-2 spike protein receptor binding domain (RBD), circumventing traditional production limitations. We screened 29 Nbs against RBD XBB.1.5 via the HDOCK server to identify a lead Nb and engineered it through computational design for heightened affinity.

2. Experimental

2.1 Selection of lead nanobody for RBD XBB.1.5

The XBB.1.5 RBD structure was prepared by changing S486 to P486 in PDB ID 8IOV. To discover a lead Nb with the highest binding affinity for the XBB.1.5 RBD target, all 29 Nbs from the Protein Data Bank (PDB) (https://www.rcsb.org/) [23] were docked with the RBD XBB.1.5 using a blind docking method in HDOCK (http://hdock.phys.hust.edu.cn/) [24]. Next, the Nb/RBD complexes underwent energy minimization using the AMBER ff14SB force field to achieve the optimal torsion of amino acid side chains [25], ensuring optimal conformations before rescoring with HDOCK. The Nb with the lowest HDOCK scores was selected as a lead Nb. This chosen Nb was then utilized in the subsequent phase of the structure-based engineering process.

2.2 Structural-based engineering of lead nanobody for RBD XBB.1.5

To improve the binding affinity of the lead Nb to RBD XBB.1.5, site-directed mutagenesis was performed on the lead Nb. In our previous study, we conducted a comprehensive benchmarking analysis to identify the most effective protein-protein docking server for RBD and Nb docking systems, utilizing a dataset of crystal structures of 29 RBD/Nb and 86 RBD/Nb complexes. Among the 7 docking tools evaluated, HDOCK demonstrated superior performance in *ab initio* docking approaches for both RBD/Nb and RBD/Ab systems [26]. Consequently, we selected HDOCK for the present study. The HDOCK score of the Nb/RBD complex from the lead Nb selection process was recorded as $HDOCK_{(Nb\ native)}$. Mutations were prioritized at residues on the Nb interface that either did not interact or had repulsive interactions with RBD XBB.1.5. Prior to redocking, each mutated amino acid was optimized using the CHARM force field within the Discovery Studio program [27]. The mutated Nb was then redocked to determine the post-mutation score, referred to as $HDOCK_{(Nb\ mutant)}$. The ΔHDOCK value for each Nb mutation was calculated to assess the binding affinity changes for each mutated residue using Equation (1) [26].

$$\Delta HDOCK = HDOCK_{(Nb\ mutant)} - HDOCK_{(Nb\ native)} \quad (1)$$

The ΔHDOCK score indicated the binding affinity of each residue of Nb to RBD XBB.1.5. The mutation that resulted in the lowest ΔHDOCK at a specific position was selected for multi-point mutation [26]. This multi-mutated Nb was then docked with RBD XBB.1.5 to obtain the final HDOCK score. The sequences of the multi-mutated Nb and the lead Nb were aligned using BioEdit software to assess sequence similarity [28].

2.3 Physicochemical properties

The predicted physicochemical properties, including contact surface amino acids, contact surface area, and chemical and physical interactions of the engineered Nb, were determined using the PDBsum server (http://www.ebi.ac.uk/thornton-srv/databases/pdbsum/Generate.html) [29]. Additionally, other properties such as molecular weight, pI value, molar extinction coefficient, instability index, aliphatic index, and grand average of hydropathicity (GRAVY) were predicted using the ProtParam (ExPASy) tool (https://web.expasy.org/ protparam/) [30]. Protein solubility was assessed using the Protein–Sol web server (https://protein-sol.manchester.ac.uk/) [31], and total charge was calculated using PROTEIN CALCULATOR v3.4 (https://protcalc.sourceforge.net/) [32]. The validation of Nb structures was conducted using MolProbity (http://molprobity.biochem.duke.edu/) [33].

3. Results and discussion

3.1 Selection of lead nanobody for RBD XBB.1.5

The selection of lead Nb for RBD XBB.1.5 was based on a docking process. The criteria for selection, the HDOCK score of the lead Nb should be low, indicating high binding affinity. This investigation discovered in Figure 1 that the Nb_7KGK exhibited the highest binding affinity (–464.97) to the targeted RBD XBB.1.5. Therefore, Nb_7KGK was appropriately chosen as the lead Nb for further amino acid engineering. This outcome aligns with earlier studies indicating that the Nb_7KGK exhibits optimal interaction with RBD Variant-of-Concern (VOC) [26].

3.2 Structural-based engineering of lead nanobody for RBD XBB.1.5

To improve the binding affinity and specificity of the Nb_7KGK, the modification of engineered Nb centered on crucial target residues at the interaction site of Nb to RBD XBB.1.5, while considering the

non-contact/interaction amino acid(s) and amino acid(s) that caused unfavorable residues upon protein-protein surface contact. In the introduction of single site-directed mutations, each mutation site was altered with various amino acids possessing diverse properties. For instance, Figure 2(a-b) illustrates that at the intriguing mutation sites of Nb_7KGK, including threonine (T33), glutamic acid (E44), alanine (A50), glycine (G55), alanine (A62), isoleucine (I98) and glutamine (Q104) were considered to mutate. We discovered that the majority of mutated residues in Nb_7KGK were aromatic residues tyrosine (Y), tryptophan (W), and histidine (H) with higher ΔHDOCK scores. Amino acid candidates were selected based on their potential to contribute to hydrophobic interactions with the RBD XBB.1.5. As a result, the engineered Nb_7KGK(7) from the multi-point mutation exhibited a more robust interaction with RBD XBB.1.5. Obviously, the HDOCK score of Nb_7KGK(7) (–604.96) indicated that the engineered Nb provided a higher binding affinity more than native Nb_7KGK. Consistently, Figure 2(b) proves that the primary characteristic of the lead Nb_7KGK was its emphasis on the complementarity-determining regions (CDRs), specifically CDRs 1-3, for engaging with the RBM of RBD XBB.1.5 [34,35]. As expected, the Nb_7KGK(7) still interact on receptor-binding motif (RBM) of RBD XBB.1.5 consistently to native Nb_7KGK (see Figure 2(c)). Moreover, Figure 3 exhibits amino acids distribution of the Nb_7KGK(7) on RBM of RBD XBB.1.5, show higher number of interface contacted residues.

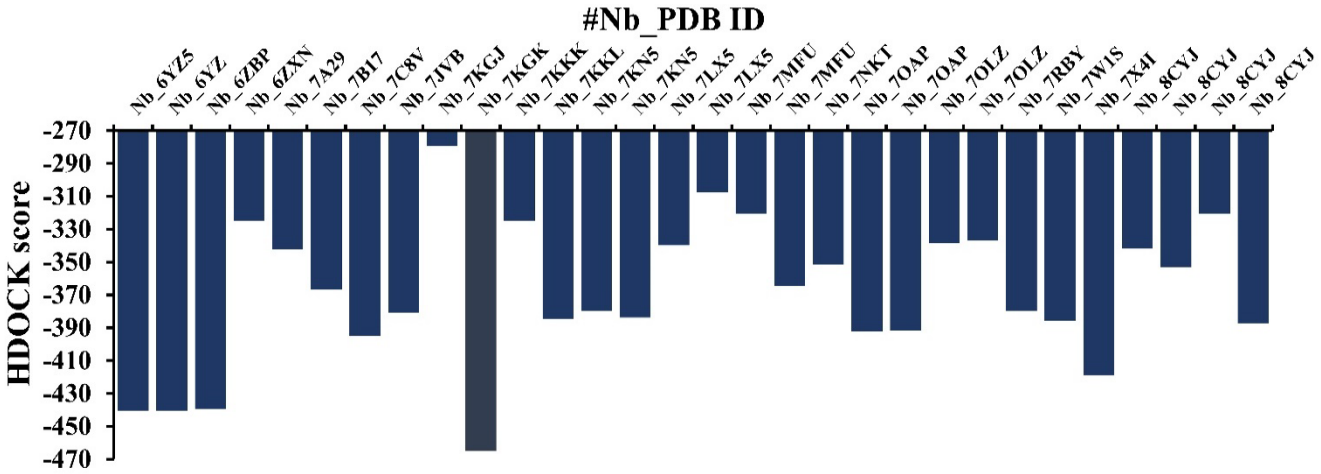

Figure 1. HDOCK score results of the docking of 29 Nbs with RBD XBB.1.5.

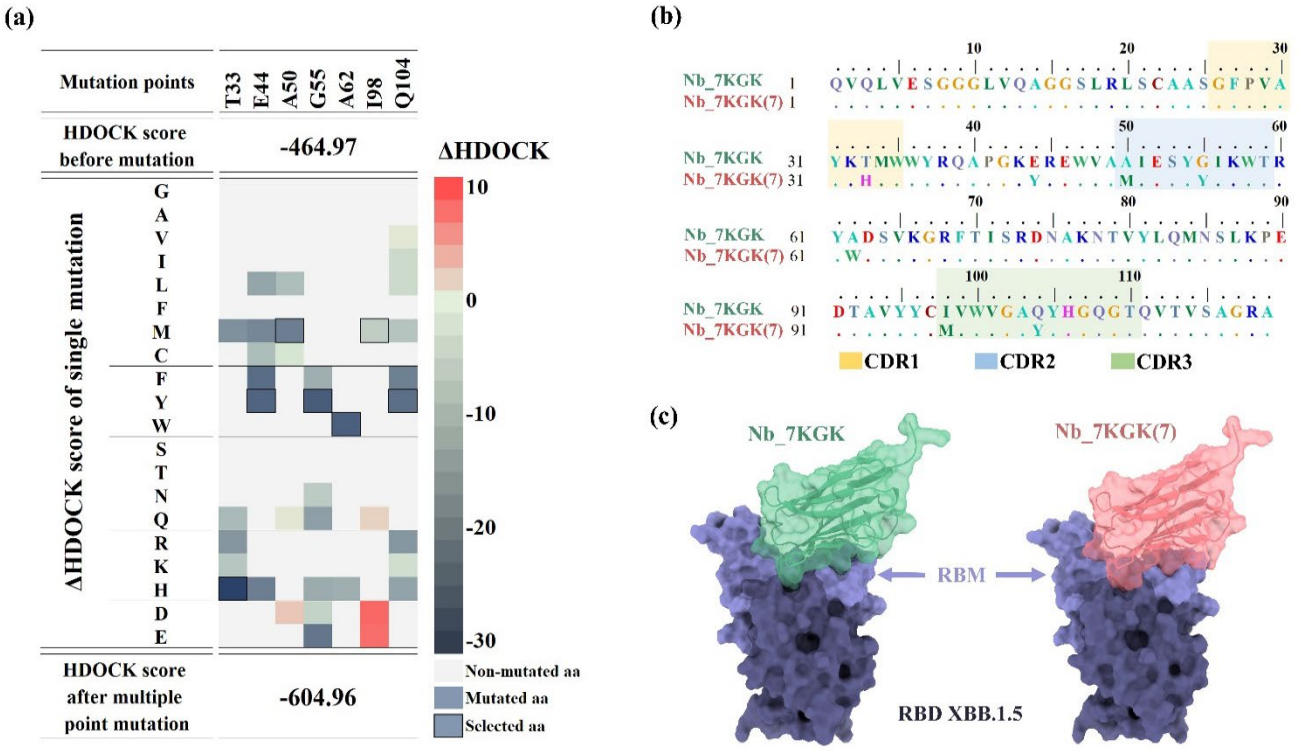

Figure 2. Mutation points of Nb_7KGK; (a) ΔHDOCK score, (b) sequence alignment of Nb_7KGK and Nb_7KGK(7), and (c) structure of docking output.

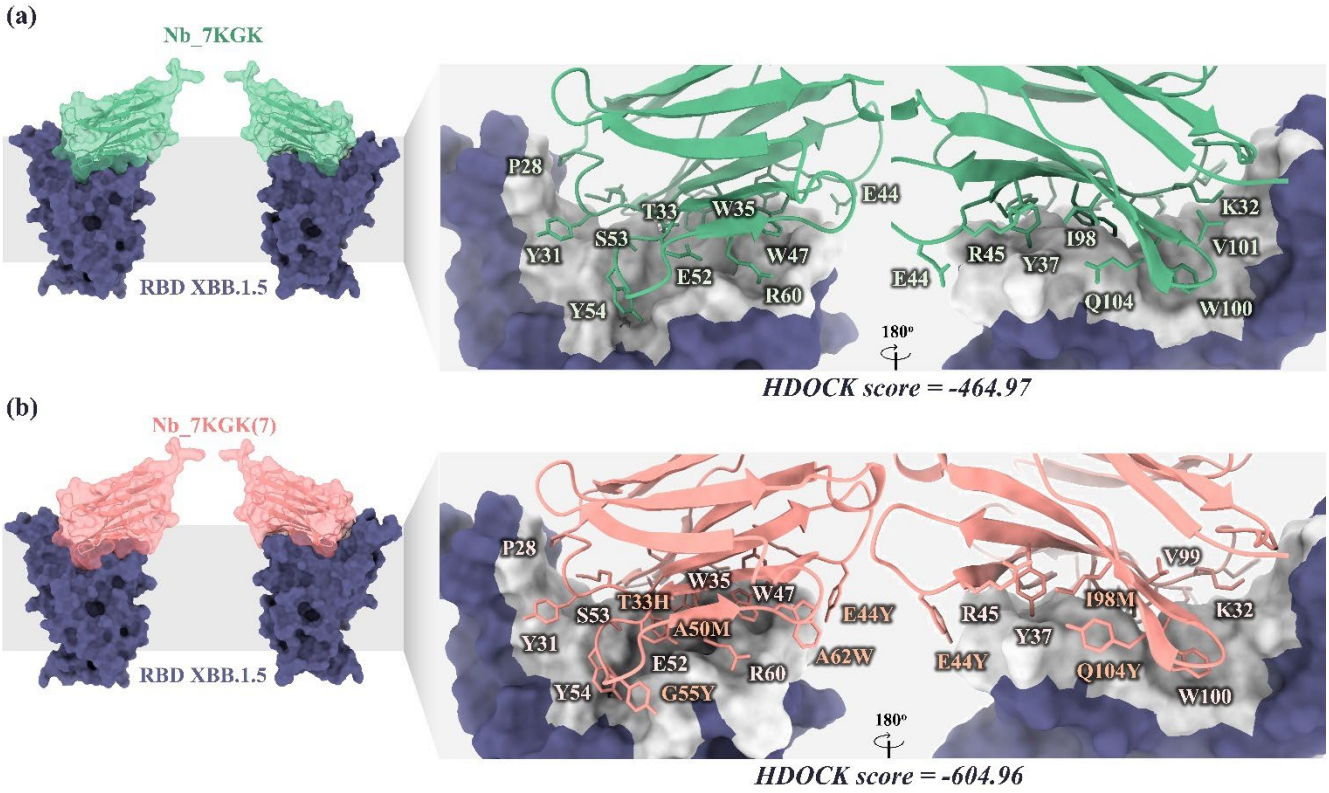

Figure 3. Distribution of interaction residues of Nb_7KGK and Nb_7KGK(7) on RBD XBB.1.5.

In addition, Figure 4 illustrates that Nb_7KGK(7) exhibited more overall interactions (a), interface residues (b), interface area (c), and a greater number of hydrogen bonds and non-bond contacts (d) in terms of chemical interactions. It is evident that the mutation residues significantly enhanced chemical interactions. For instance, T33H, A50M, I98M, and Q104Y significantly improved hydrogen bond interactions, while E44Y, A50M, and A62W meaningfully increased non-bond contact interactions. These findings align with previous studies that identified hydrophobic interactions from aromatic residues as a key interaction of Nb on the RBM of RBD [36,37]. Notably, the mutated residues were predominantly located within CDR1 (T33H), CDR2 (G55Y), and CDR3 (I98M and Q104Y). These are essential structural features facilitating binding to the target ligand [34,35]

Furthermore, Figure 5 demonstrates that Nb_7KGK(7) interacts more strongly with RBD XBB.1.5 (HDOCK score –604.96) than human ACE2 (HDOCK score –305.14). This discovery indicated that Nb_7KGK(7) exhibits a robust interaction with RBD, surpassing its interaction strength with ACE2 [38,39]. We suggest that the engineered Nb could potentially be developed as a new neutralizing Nb for the protection or treatment of SARS-CoV-2 XBB.1.5 infection [40,41].

3.3 Physicochemical properties

According to predictions of physicochemical properties in Table 1, the engineered Nb_7KGK(7) exhibited only minor alterations in its overall characteristics compared to its original form, Nb_7KGK. Replacing the aliphatic residues in the native Nb with aromatic residues (G55Y and A62W) led to a slightly decrease in the aliphatic index. In contrast, aromatic mutations (T33H, E44Y, G55Y, A62W, and Q104Y) increased the molar extinction coefficient at 280 nm, thereby imparting a distinctive trait to the novel Nb [42]. Although the engineered Nb_7KGK(7) has a higher aromatic residue content, the histidine substitution at T33H enhanced polarity (resulting in a more negative GRAVY) and total charge at biological pH, thereby increasing the pI value [43]. Typically, nanobodies exhibit a basic pI value and a high positive charge as a common trend, strategically designed to mitigate self-aggregation [34]. Since mutations were distributed across seven residues, all mutation residues preserved the solubility of Nb_7KGK(7).

The evaluation of the designed Nb_7KGK(7) against the native Nb_7KGK from the PDB reveals differences in structural quality based on Clashscore, Ramachandran Z-score, and MolProbity score. Nb_7KGK(7) demonstrates superior performance in Clashscore, achieving a perfect score of 0 (100th percentile) compared to Nb_7KGK's 3.79 (96th percentile), indicating the absence of steric clashes in the designed model. The Ramachandran Z-score, which evaluates deviations in backbone dihedral angles, highlights issues in both models. Nb_7KGK scores -3.94 ± 0.62, while Nb_7KGK(7) shows a slight improvement to -3.02 ± 0.78; however, both scores exceed the acceptable threshold ($|Z\text{-score}|<2$), indicating significant backbone geometry challenges. The MolProbity score, a comprehensive quality measure, favors Nb_7KGK(7) at 1.73 (88th percentile) over Nb_7KGK at 2.48 (48th percentile), reflecting enhanced overall structural quality [44]. These improvements suggest better atomic packing and geometry in Nb_7KGK(7) compared to the native Nb.

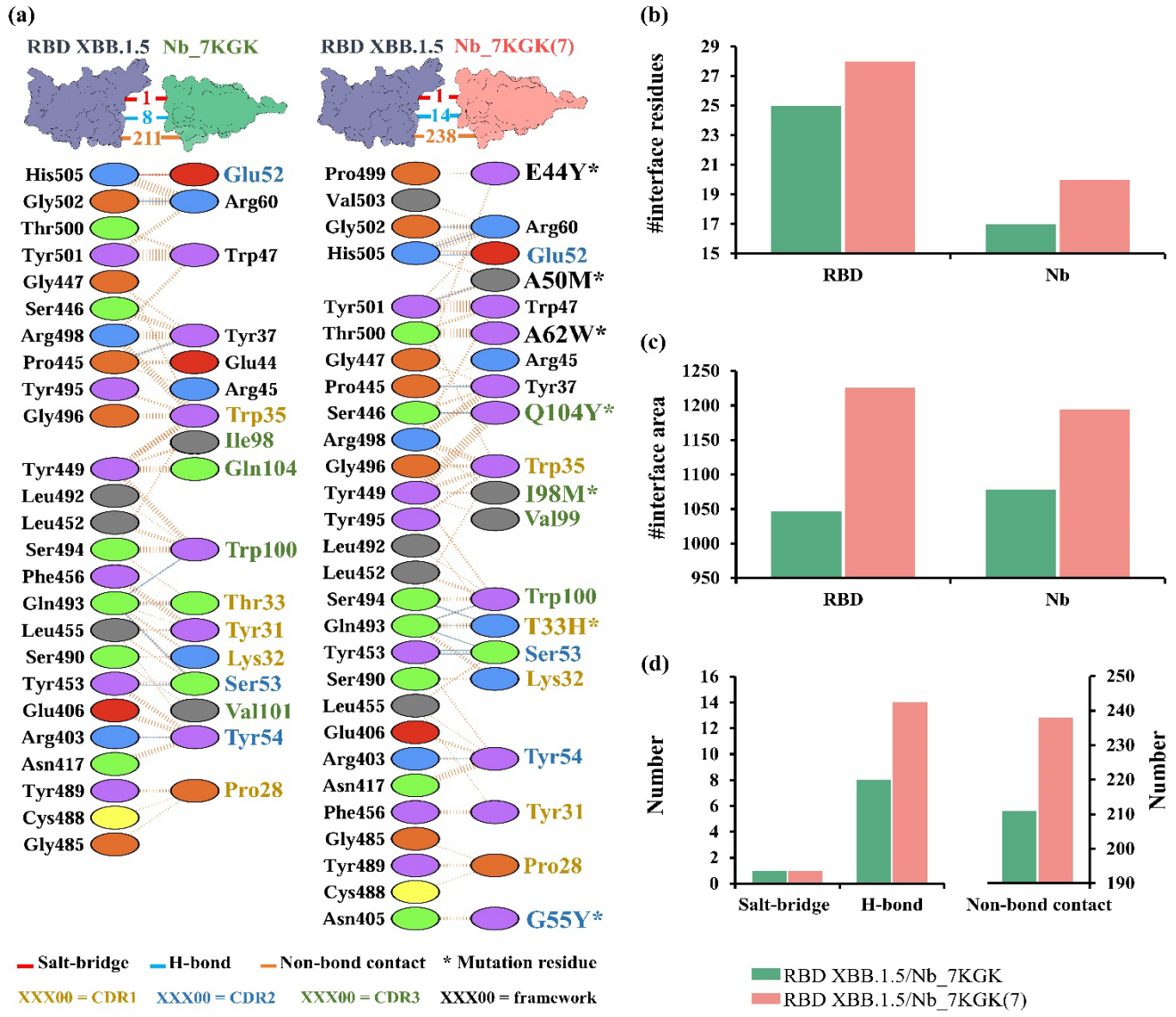

Figure 4. The comparison of protein-protein interactions of (a) Nb_7KGK and Nb_7KGK(7) with RBD XBB.1.5, (b) interface residue, (c) interface area, and (d) chemical interactions of RBD XBB.1.5/Nb_7KGK and RBD XBB.1.5/Nb_7KGK(7).

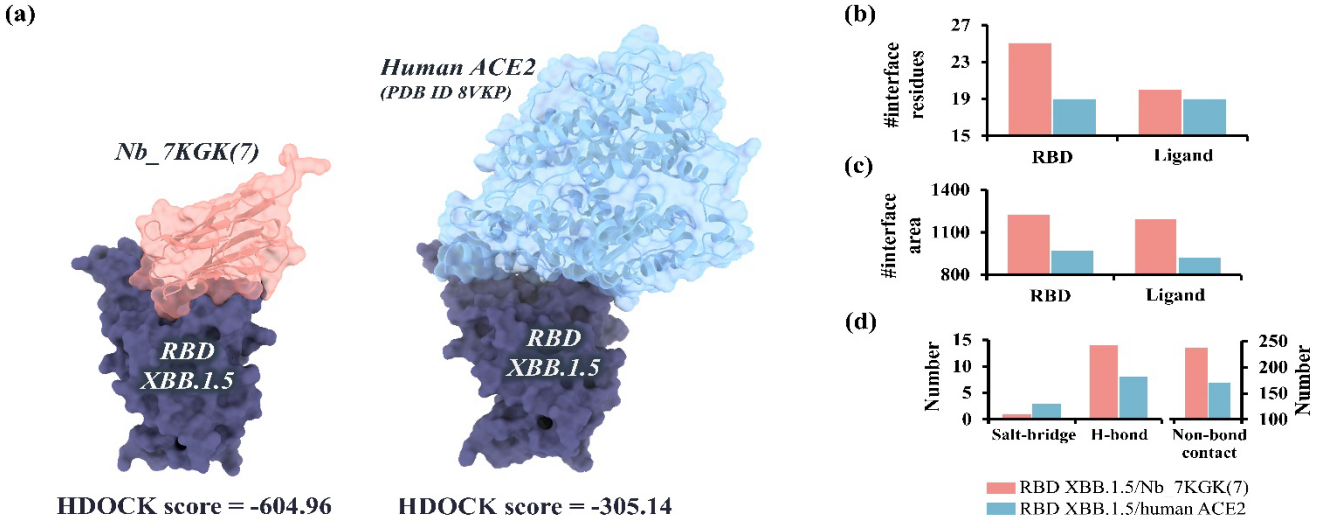

Figure 5. The comparison of (a) HDOCK score and binding posture, and the protein-protein interaction parameters; (b) interface residue, (c) interface area, and (d) chemical interactions of RBD XBB.1.5/Nb_7KGK(7) and RBD XBB.1.5/human ACE2.

Table 1. Physicochemical properties of Nb_7KGK and Nb_7KGK(7).

Physicochemical properties	Nb_7KGK	Nb_7KGK(7)
Number of amino acids	119	119
Formula weight	13144.88	13549.42
Aliphatic index	72.94	67.98
Ext. coefficient (at 280 nm, disulfide forms)	39420	49515
Grand average of hydropathicity (GRAVY)	–0.274	–0.309
Total charge at pH 7.4	4.7	5.8
pI value	9.36	9.42
Solubility	0.61	0.61

4. Conclusions

The selection of the lead Nb for RBD XBB.1.5 was based on a docking process, aiming for a low HDOCK score indicating high binding affinity. Nb_7KGK exhibited the highest binding affinity, making it the lead Nb for further engineering. The Nb_7KGK(7) was engineered through multiple point mutations focusing on key residues, showing enhanced interaction with RBD XBB.1.5 and surpassing the native Nb_7KGK in binding affinity. This engineered Nb displayed stronger interaction with RBD XBB.1.5 compared to human ACE2, indicating its potential as a neutralizing agent against SARS-CoV-2 XBB.1.5. The physicochemical property predictions of Nb_7KGK(7) showed improved properties, such as an increased molar extinction coefficient and pI value, while maintaining good solubility.

Acknowledgement

This research project is supported by King Mongkut's University of Technology Thonburi (KMUTT), Thailand Science Research and Innovation (TSRI), and National Science, Research and Innovation Fund (NSRF) (Fiscal year 2025, Grant number FRB680074/0164). P. L. would like to thank the Petchra Pra Jom Klao Ph.D. Research Scholarship from King Mongkut's University of Technology Thonburi. N. K. thanks the Second Century Fund (C2F), Chulalongkorn University, for a Ph.D. Scholarship. T.R. would like to thank the National Research Council of Thailand (NRCT) (Grant number N42A650231).

References

[1] T. Sharma, B. Gerstman, and P. Chapagain, "Distinctive features of the XBB.1.5 and XBB.1.16 spike protein receptor-binding domains and their roles in conformational changes and angiotensin-converting enzyme 2 binding," *International Journal of Molecular Sciences,* vol. 24, no. 16, p. 12586, 2023.

[2] K. Uriu, J. Ito, J. Zahradnik, S. Fujita, Y. Kosugi, G. Schreiber, and K. Sato, "Enhanced transmissibility, infectivity, and immune resistance of the SARS-CoV-2 omicron XBB.1.5 variant," *The Lancet Infectious Diseases,* vol. 23, no. 3, pp. 280-281, 2023.

[3] C. Yue, W. Song, L. Wang, F. Jian, X. Chen, F. Gao, Z. Shen, Y. Wang, X. Wang, and Y. Cao, "Enhanced transmissibility of XBB.1.5 is contributed by both strong ACE2 binding and antibody evasion," *bioRxiv*, p. 522427, 2023.

[4] D. V. Parums, "The XBB. 1.5 ('Kraken') subvariant of omicron SARS-CoV-2 and its rapid global spread," *Medical science monitor: international medical journal of experimental and clinical research,* vol. 29, pp. e939580-1, 2023.

[5] A. Sugano, H. Kataguchi, M. Ohta, Y. Someya, S. Kimura, Y. Maniwa, T. Tabata, and Y. Takaoka, "SARS-CoV-2 omicron XBB. 1.5 may be a variant that spreads more widely and faster than other variants," *bioRxiv*, p. 524660, 2023.

[6] B. Ju, Q. Zhang, J. Ge, R. Wang, J. Sun, X. Ge, J. Yu, S. Shan, B. Zhou, and S. Song, "Human neutralizing antibodies elicited by SARS-CoV-2 infection," *Nature,* vol. 584, no. 7819, pp. 115-119, 2020.

[7] D. Ray, R. N. Quijano, and I. Andricioaei, "Point mutations in SARS-CoV-2 variants induce long-range dynamical perturbations in neutralizing antibodies," *Chemical science,* vol. 13, no. 24, pp. 7224-7239, 2022.

[8] T. Zhou, L. Wang, J. Misasi, A. Pegu, Y. Zhang, D. R. Harris, A. S. Olia, C. A. Talana, E. S. Yang, M. Chen, M. Choe, W. Shi, I-T. Teng, A. Creanga, C. Jenkins, K. Leung, T. Liu, E.-S. D. Stancofski, T. Stephens, B. Zhang, Y. Tsybovsky, B. S. Graham, J. R. Mascola, N. J. Sullivan, P. D. Kwong, "Structural basis for potent antibody neutralization of SARS-CoV-2 variants including B.1.1.529," *Science,* vol. 376, no. 6591, pp. eabn8897, 2022.

[9] E. V. Capela, M. R. Aires-Barros, M. G. Freire, and A. M. Azevedo, "Monoclonal antibodies—addressing the challenges on the manufacturing processing of an advanced class of therapeutic agents," *Frontiers in Clinical Drug Research - Anti Infectives,* vol. 4, no. 4, pp. 142, 2017.

[10] C. Ackaert, N. Smiejkowska, C. Xavier, Y. G. Sterckx, S. Denies, B. Stijlemans, Y. Elkrim, N. Devoogdt, V. Caveliers, and T. Lahoutte, "Immunogenicity risk profile of nanobodies," *Frontiers in immunology,* vol. 12, p. 632687, 2021.

[11] J. Huo, A. Le Bas, R. R. Ruza, H. M. Duyvesteyn, H. Mikolajek, T. Malinauskas, T. K. Tan, P. Rijal, M. Dumoux, and P. N. Ward, "Neutralizing nanobodies bind SARS-CoV-2 spike RBD and block interaction with ACE2," *Nature structural & molecular biology,* vol. 27, no. 9, pp. 846-854, 2020.

[12] G. Van Heeke, K. Allosery, V. De Brabandere, T. De Smedt, L. Detalle, and A. de Fougerolles, "Nanobodies® as inhaled biotherapeutics for lung diseases," *Pharmacology & Therapeutics,* vol. 169, pp. 47-56, 2017.

[13] Z. R. Crook, N. W. Nairn, and J. M. Olson, "Miniproteins as a powerful modality in drug development," *Trends in Biochemical Sciences,* vol. 45, no. 4, pp. 332-346, 2020.

[14] F. Y. Frejd, and K.-T. Kim, "Affibody molecules as engineered protein drugs," *Experimental & Molecular Medicine,* vol. 49, no. 3, p. e306, 2017.

[15] E. L. Hesketh, C. Tiede, H. Adamson, T. L. Adams, M. J. Byrne, Y. Meshcheriakova, I. Kruse, M. J. McPherson, G. P. Lomonossoff, D. C. Tomlinson, and N. A. Ranson, "Affimer reagents as tools in diagnosing plant virus diseases," *Scientific Reports,* vol. 9, no. 1, p. 7524, 2019.

[16] O. Hantschel, "Monobodies as possible next-generation protein therapeutics - a perspective," *Swiss Medical Weekly,* vol. 147, no. 47, p. 14545, 2017.

[17] Y. Xiang, S. Nambulli, Z. Xiao, H. Liu, Z. Sang, W. P. Duprex, D. Schneidman-Duhovny, C. Zhang, and Y. Shi, "Versatile and multivalent nanobodies efficiently neutralize SARS-CoV-2," *Science,* vol. 370, no. 6523, pp. 1479-1484, 2020.

[18] M. Aksu, P. Kumar, T. Güttler, W. Taxer, K. Gregor, B. Mußil, O. Rymarenko, K. M. Stegmann, A. Dickmanns, S. Gerber, W. Reineking, C. Schulz, T. Henneck, A. Mohamed, G. Pohlmann, M. Ramazanoglu, K. Mese, U. Groß, T. Ben-Yedidia, O. Ovadia, D. W. Fischer, M. Kamensky, A. Reichman, W. Baumgärtner, M. von Köckritz-Blickwede, M. Dobbelstein, and D. Görlich, "Nanobodies to multiple spike variants and inhalation of nanobody-containing aerosols neutralize SARS-CoV-2 in cell culture and hamsters," *Antiviral Research,* vol. 221, p. 105778, 2024.

[19] J. Wang, B. Shi, H. Chen, M. Yu, P. Wang, Z. Qian, K. Hu, and J. Wang, "Engineered multivalent nanobodies efficiently neutralize SARS-CoV-2 omicron subvariants BA.1, BA.4/5, XBB.1 and BQ.1.1," *Vaccines (Basel),* vol. 12, no. 4, 2024.

[20] G. Zhong, S. Xu, M. Cui, Q. Dong, X. Wang, Q. Xia, J. Gao, Y. Pei, Y. Qiao, and G. Pastel, "Rapid, high-temperature, in situ microwave synthesis of bulk nanocatalysts," *Small,* vol. 15, no. 47, p. 1904881, 2019.

[21] V. Salema, and L. Á. Fernández, "Escherichia coli surface display for the selection of nanobodies," *Microbial biotechnology,* vol. 10, no. 6, pp. 1468-1484, 2017.

[22] Y.-J. Che, H.-W. Wu, L.-Y. Hung, H.-Y. Chang, K. Wang, and G.-B. Lee, "An integrated microfluidic system for screening of peptides specific to colon cancer cells and colon cancer stem cells using the phage display technology," vol. 5, no. 9. pp. 440-443, 2015.

[23] S. K. Burley, H. M. Berman, G. J. Kleywegt, J. L. Markley, H. Nakamura, and S. Velankar, "Protein Data Bank (PDB): the single global macromolecular structure archive," *Protein crystallography: methods and protocols*, pp. 627-641, 2017.

[24] Y. Yan, H. Tao, J. He, and S.-Y. Huang, "The HDOCK server for integrated protein–protein docking," *Nature protocols,* vol. 15, no. 5, pp. 1829-1852, 2020.

[25] J. A. Maier, C. Martinez, K. Kasavajhala, L. Wickstrom, K. E. Hauser, and C. Simmerling, "ff14SB: improving the accuracy of protein side chain and backbone parameters from ff99SB," *Journal of chemical theory and computation,* vol. 11, no. 8, pp. 3696-3713, 2015.

[26] P. Longsompurana, T. Rungrotmongkol, N. Plongthongkum, K. Wangkanont, P. Wolschann, and R. P. Poo-Arporn, "Computational design of novel nanobodies targeting the receptor binding domain of variants of concern of SARS-CoV-2," *Plos one,* vol. 18, no. 10, p. e0293263, 2023.

[27] R. B. Best, X. Zhu, J. Shim, P. E. Lopes, J. Mittal, M. Feig, and A. D. MacKerell Jr, "Optimization of the additive CHARMM all-atom protein force field targeting improved sampling of the backbone ϕ, ψ and side-chain $\chi 1$ and $\chi 2$ dihedral angles," *Journal of chemical theory and computation,* vol. 8, no. 9, pp. 3257-3273, 2012.

[28] H.-F. Tippmann, "Analysis for free: Comparing programs for sequence analysis," *Briefings in bioinformatics,* vol. 5, no. 1, pp. 82-87, 2004.

[29] R. A. Laskowski, J. Jabłońska, L. Pravda, R. S. Vařeková, and J. M. Thornton, "PDBsum: Structural summaries of PDB entries," *Protein science,* vol. 27, no. 1, pp. 129-134, 2018.

[30] E. Gasteiger, C. Hoogland, A. Gattiker, S. e. Duvaud, M. R. Wilkins, R. D. Appel, and A. Bairoch, *Protein identification and analysis tools on the ExPASy server*: Springer, 2005.

[31] M. Hebditch, M. A. Carballo-Amador, S. Charonis, R. Curtis, and J. Warwicker, "Protein–sol: A web tool for predicting protein solubility from sequence," *Bioinformatics,* vol. 33, no. 19, pp. 3098-3100, 2017.

[32] R. Deller, B. Carter, I. Zampetakis, F. Scarpa, and A. Perriman, "The effect of surface charge on the thermal stability and ice recrystallization inhibition activity of antifreeze protein III (AFP III)," *Biochemical and biophysical research communications,* vol. 495, no. 1, pp. 1055-1060, 2018.

[33] I. W. Davis, A. Leaver-Fay, V. B. Chen, J. N. Block, G. J. Kapral, X. Wang, L. W. Murray, W. B. Arendall, 3rd, J. Snoeyink, J. S. Richardson, and D. C. Richardson, "MolProbity: All-atom contacts and structure validation for proteins and nucleic acids," *Nucleic Acids Research,* vol. 35, pp. W375-83, 2007.

[34] Z. Zhong, Y. Yang, X. Chen, Z. Han, J. Zhou, B. Li, and X. He, "Positive charge in the complementarity-determining regions of synthetic nanobody prevents aggregation," *Biochemical and Biophysical Research Communications,* vol. 572, pp. 1-6, 2021.

[35] M. L. Fernández-Quintero, E. F. DeRose, S. A. Gabel, G. A. Mueller, and K. R. Liedl, "Nanobody paratope ensembles in solution characterized by MD simulations and NMR," *International Journal of Molecular Sciences,* vol. 23, no. 10, p. 5419, 2022.

[36] J. Lan, J. Ge, J. Yu, S. Shan, H. Zhou, S. Fan, Q. Zhang, X. Shi, Q. Wang, and L. Zhang, "Structure of the SARS-CoV-2 spike receptor-binding domain bound to the ACE2 receptor," *Nature,* vol. 581, no. 7807, pp. 215-220, 2020.

[37] Y. Wang, M. Liu, and J. Gao, "Enhanced receptor binding of SARS-CoV-2 through networks of hydrogen-bonding and hydrophobic interactions," *Proceedings of the National Academy of Sciences,* vol. 117, no. 25, pp. 13967-13974, 2020.

[38] T. R. Wagner, E. Ostertag, P. D. Kaiser, M. Gramlich, N. Ruetalo, D. Junker, J. Haering, B. Traenkle, M. Becker, and A. Dulovic, "NeutrobodyPlex—monitoring SARS-CoV-2 neutralizing immune responses using nanobodies," *EMBO reports,* vol. 22, no. 5, p. e52325, 2021.

[39] S. He, J. Wang, H. Chen, Z. Qian, K. Hu, B. Shi, and J. Wang, "A competitive panning method reveals an anti-SARS-CoV-2 nanobody specific for an RBD-ACE2 binding site," *Vaccines,* vol. 11, no. 2, p. 371, 2023.

[40] X. Wu, L. Cheng, M. Fu, B. Huang, L. Zhu, S. Xu, H. Shi, D. Zhang, H. Yuan, and W. Nawaz, "A potent bispecific nanobody protects hACE2 mice against SARS-CoV-2 infection via intranasal administration," *Cell reports,* vol. 37, no. 3, 2021.

[41] K. C. Entzminger, J. K. Fleming, P. D. Entzminger, L. Y. Espinosa, A. Samadi, Y. Hiramoto, S. C. Okumura, and T. Maruyama, "Rapid engineering of SARS-CoV-2 therapeutic antibodies to increase breadth of neutralization including BQ. 1.1, CA. 3.1, CH. 1.1, XBB. 1.16, and XBB. 1.5," *Antibody Therapeutics,* vol. 6, no. 2, pp. 108-118, 2023.

[42] P. P. Pawar, and G. K. Bichile, "Molar extinction coefficients of some proteins," *Archives of Physics Research,* vol. 2, no. 4, pp. 50-59, 2011.

[43] B. M. Huyghues-Despointes, R. L. Thurlkill, M. D. Daily, D. Schell, J. M. Briggs, J. M. Antosiewicz, C. N. Pace, and J. M. Scholtz, "pK values of histidine residues in ribonuclease Sa: effect of salt and net charge," *Journal of molecular biology,* vol. 325, no. 5, pp. 1093-1105, 2003.

[44] O. V. Sobolev, P. V. Afonine, N. W. Moriarty, M. L. Hekkelman, R. P. Joosten, A. Perrakis, and P. D. Adams, "A global ramachandran score identifies protein structures with unlikely stereochemistry," *Structure,* vol. 28, no. 11, pp. 1249-1258.e2, 2020.